ENERGY DEMAND REDUCTION DUE TO AN INTELLIGENT SHADING CONTROL STRATEGY

P. Klanatsky[1], H. Plank[1] and C. Heschl[1, 2]
[1]Fachhochschule Burgenland GmbH, University of Applied Sciences, Department Energy and Environmental Management, Pinkafeld, Austria
[2]Forschung Burgenland GmbH, Center for Building Technology, Pinkafeld, Austria

ABSTRACT

The energy efficiency of buildings with large glass façades depends strongly on their shading design. Particularly the applied shading control strategy plays an decisive role if surface heating and cooling systems with a large thermal inertia are used for demand side management objectives. Hence, a comprehensive, intelligent control strategy which considers all relevant HVAC subsystems is needed to facilitate the decarbonisation of the European power supply. Such an intelligent control strategy was developed for thermally activated building systems and external shading devices. It was validated for a "living laboratory" building under real operating conditions over two years. Results show that a significant reduction of the energy demand for the static cooling surfaces of about 70% was achieved with a simultaneous reduction ot the complaints about high room air temperatures.

Keywords: shading device, blinds, control strategy

INTRODUCTION

For office buildings with large glass façades, the cooling demand depends strongly on the incident solar radiation (Planas et al., 2018). Furthermore, parameters such as type of glass (insulated glass units, selective glazing systems, etc.) and the external shading technology that is in place are key drivers of cooling demand (Westphal and Andreis, 2016). The operation of the shading devices to reduce the incident solar radiation through a glass façade can also take into account the balance between daylighting and energy consumption (Tzempelikos and Shen, 2011; Sagerschnig et al., 2010).

In the European Union, the gross energy consumption required for heating and cooling stands at a staggering 50% of total energy needs with 80% of this portion consumed by buildings alone. It is therefore crucial to accelerate the efforts laid out in the EUs Energy Performance of Buildings Directive (EPBD) to achieve the EU Commission's Energy 2030 targets (European Commission, 2018).

In order to study the energy savings potential of an office building with glass façades and with static heating and cooling surfaces, an investigation was carried out using a "living laboratory" (office building operating under real user conditions). Preliminary findings indicated that the heating and cooling strategy for the buildings surfaces was not ideal and incoherent with the other installed systems within the building such as the shading system/ shading blinds on the outside of the glass façades. Moreover, the building occupants complained of abnormally high room air temperatures (primarily in rooms located in the South and West of the building) and about the permanent disruption brought about by the changing of the position of the external shading devices (noise pollution by the servomotors). A survey conducted by Fuetterer et al. (2017) confirmed the findings of Waide (2013) that a high fraction of building automation systems have faults/defects or errors, caused by poor design of the systems during the planning stage, rushed installation procedures leading to incorrect installation and commissioning, inadequate inspection and review and also handling errors after post-commissioning.

METHODOLOGY

Analyzed Object

For these investigations, the office building of the Forschung Burgenland GmbH in Pinkafeld, the ENERGETIKUM (Figure 1) was used.

Figure 1: ENERGETIKUM from the point of view of South-West

The ENERGETIKUM is two-story building (with 601.2 m² main usable area) that also serves as a living laboratory, which means that research is done while the building is concurrently used on an everyday basis as office space. The office complex was built in the

DOI: 10.3217/978-3-85125-786-1-40

year 2014 and attained full occupancy in 2015. The energy performance indicators of the office complex for heating and cooling (energy performance certificate - asset rating) are listed in table 1.

Table 1:
Energy performance indicators of the energy demand for space heating and cooling

Space heating	Space cooling
46.75 kWh/(m²a)	26.43 kWh/(m²a)

Building Envelope and Glazing / Shading

While the east and the north side of the office building consist of insulated reinforced concrete, the building envelope on the south and the west side consist of a triple glazing façade. The ground floor façade has external shading devices (blinds), which are integrated in the building automation control system and also internal manually operated shading devices (vertical blinds). The upper floor has external shading devices (blinds) and also internal shading devices (roller blinds). Both are integrated in the building automation control system.

Technical building equipment

Only the most important technical building equipments which pertain directly to this study are described here. For space heating and cooling with a reversible heat pump three different static heating/ cooling surfaces can be activated: the floor; a near surface heating/cooling system in the ceiling and also a concrete core activation of the ceiling. An air conditioning system is used to ensure hygienic air exchange rates.

Systematic approach

The starting point of this work was an analysis of the operation mode and also of the set values of the supply temperatures of the static heating and cooling surfaces. Also the room air temperatures in the thermal zones and the air conditioning system were analysed. It could be determined that in the winter months the air temperature in some office rooms reached more than 26°C. Cosequently the near surface cooling system in the ceiling and the thermal activation of the building structure were active throughout the day. The analysis also demonstrated that for both systems in the ceiling, different set values of the inlet temperatures of the fluid were considered. In the night that followed, the floor heating system was activated because of the room cooling down due to the low outside air temperature. Also the building occupants were dissatisfied with the control strategies of the other systems (like external shading devices and the volume flow rates of the supply air in the thermal zone). Because the air conditioning system operated most of the time at partial load (24/7), the control behaviour of the preheater, the cooling register and also of the reheater was not ideal. On the basis of these preliminary results, the following measures were taken:

- Installation of a weather station on the building's flat roof surface to measure the prevailing climatic conditions (Plank et al., 2019).
- Implementation of a cloud-based measurement data acquisition system to collect all operating data of the building automation system.
- Full integration of the external and internal shading devices in the building automation and control system.
- Development of a BACnet-Open Platform Communication (OPC)-Matlab user interface to read and write data from or to devices of the building control system (see Figure 2). The BACnet-OPC-Matlab user interface also includes the control strategies for the heating and cooling surfaces, for the external shading devices and for the hygienic air change for all thermal zones.
- Manual optimization of the control parameters for the preheater, the cooling register and the reheater of the air conditioning system and the defining of a time schedule for the operating hours.
- Evaluation of the energy demand by using the developed BACnet-OPC-Matlab user interfaces and control strategies.

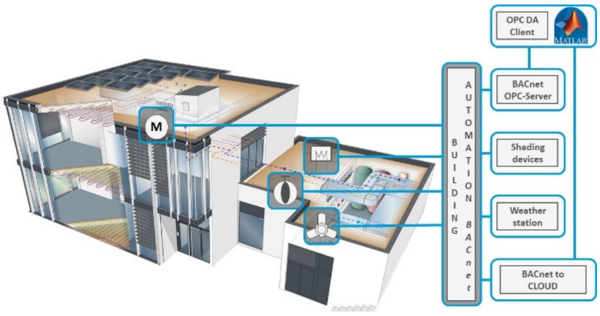

Figure 2: Extension of the BACnet and integration of the BACnet-OPC-Matlab user interface

The following sections describe the activities undertaken in detail and the impact of these measures.

MATLAB USER-INTERFACE

Communication between the BACnet and Matlab can be maintained by using an BACnet OPC Server and the OPC toolbox in Matlab. In the next subsections the Matlab user interface with graphical user interfaces for space heating and cooling, hygienic air change and external shading devices will be explained.

DOI: 10.3217/978-3-85125-786-1-40

Space heating and cooling

For space heating and cooling, the following thermally activated building systems can be used:

- Floor heating/cooling system (short name: FBH).
- Near surface heating/cooling system in the ceiling (short name: BKAON).
- Heating/cooling system in the concrete core in the ceiling (short name: BKA).

Depending on the operating mode of the distributor (warm/cold), the system for space heating (red: FBH) and also for space cooling (blue: BKAON) can be chosen in the graphical user interface (see Figure 3).

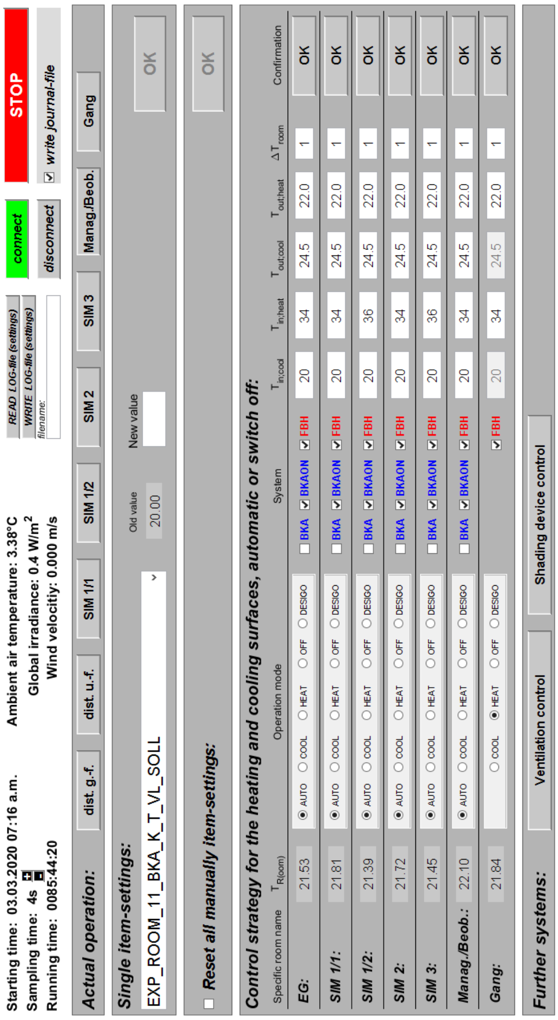

Starting time: 03.03.2020 07:16 a.m.
Sampling time: 4s
Running time: 0085:44:20

Ambient air temperature: 3.38°C
Global irradiance: 0.4 W/m²
Wind velocitiy: 0.000 m/s

Actual operation:

Single item-settings:

EXP_ROOM_11_BKA_K_T_VL_SOLL

Old value: 20.00

New value:

☐ **Reset all manually item-settings:**

Control strategy for the heating and cooling surfaces, automatic or switch off:

Specific room name	$T_{R(room)}$	Operation mode	System	$T_{in;cool}$	$T_{in;heat}$	$T_{out;cool}$	$T_{out;heat}$	ΔT_{room}	Confirmation
EG:	21.53	● AUTO ○ COOL ○ HEAT ○ OFF ○ DESIGO	☐ BKA ☑ BKAON ☑ FBH	20	34	24.5	22.0	1	OK
SIM 1/1:	21.81	● AUTO ○ COOL ○ HEAT ○ OFF ○ DESIGO	☐ BKA ☑ BKAON ☑ FBH	20	34	24.5	22.0	1	OK
SIM 1/2:	21.39	● AUTO ○ COOL ○ HEAT ○ OFF ○ DESIGO	☐ BKA ☑ BKAON ☑ FBH	20	36	24.5	22.0	1	OK
SIM 2:	21.72	● AUTO ○ COOL ○ HEAT ○ OFF ○ DESIGO	☐ BKA ☑ BKAON ☑ FBH	20	34	24.5	22.0	1	OK
SIM 3:	21.45	● AUTO ○ COOL ○ HEAT ○ OFF ○ DESIGO	☐ BKA ☑ BKAON ☑ FBH	20	36	24.5	22.0	1	OK
Manag./Beob.:	22.10	● AUTO ○ COOL ○ HEAT ○ OFF ○ DESIGO	☐ BKA ☑ BKAON ☑ FBH	20	34	24.5	22.0	1	OK
Gang:	21.84	○ COOL ● HEAT ○ OFF ○ DESIGO	☑ FBH	20	34	24.5	22.0	1	OK

Further systems:

Figure 3: GUI of the developed BACnet-OPC-Matlab user interface for controlling the heating and cooling surfaces

Figure 4 shows the implemented control strategy (two-point controllers) of these systems for heating and cooling (and also for automatically operation between heating and cooling).

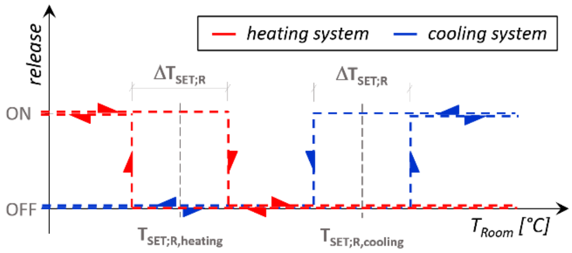

Figure 4: Control strategy of the surface heating and cooling surfaces

Hygienic air change

The operation mode of the air conditioning system is set to guarantee a hygienic air exchange rate in the thermal zones. To control the volume flowrate of the supply air in each thermal zone, a two-point controller was considered for each volumetric flow controller (see Figure 5). In an additional graphical user interface for ventilation (similar to that in Figure 3) the necessary parameters are defined as user inputs for each thermal zone.

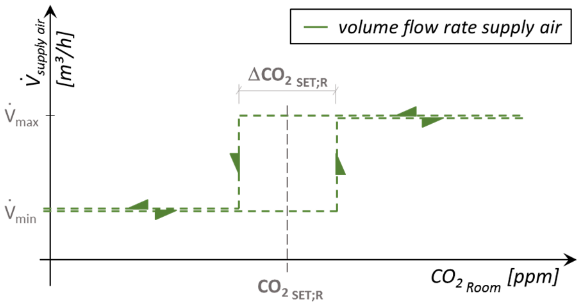

Figure 5: Control strategy of the volume flow rate of the supply air

Furthermore, the control parameters for the water/air heat exchangers and the set value for dehumidification (cooling register) of the air conditioning system were adapted and a schedule for the operating hours was implemented. Also, the control variable of the humidity of the exhaust air was changed from relative humidity to absolute humidity.

External shading devices (blinds)

To control the incident solar radiation, the external shading devices can be used. In each thermal zone the different oriented devices can be adjusted using two parameters. The first parameter to adjust the external shading device is the height of shading and the second is the slat angle of the blinds (see Figure 6).

In Figure 7, the flow chart of the intelligent control strategy is displayed. As the flow chart shows, the control strategy of the external shading devices is changing with the operational mode of the space heating and cooling systems (see also Klanatsky et al. (2019a) and Klanatsky et al. (2019b)).

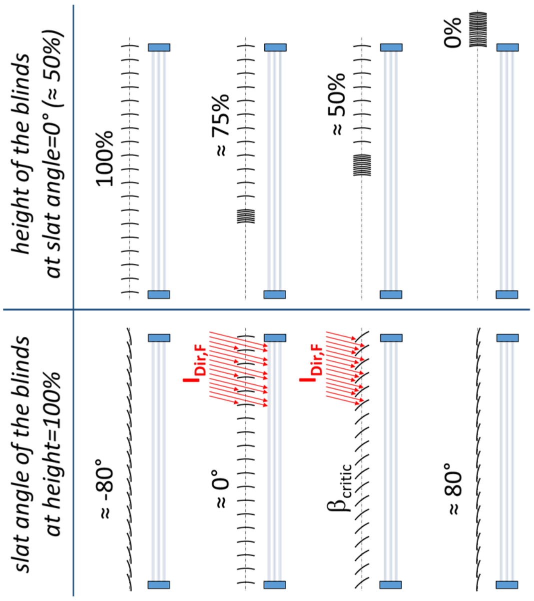

Figure 6: Impact of the parameter "height" and "slat angle" on the position of the blinds

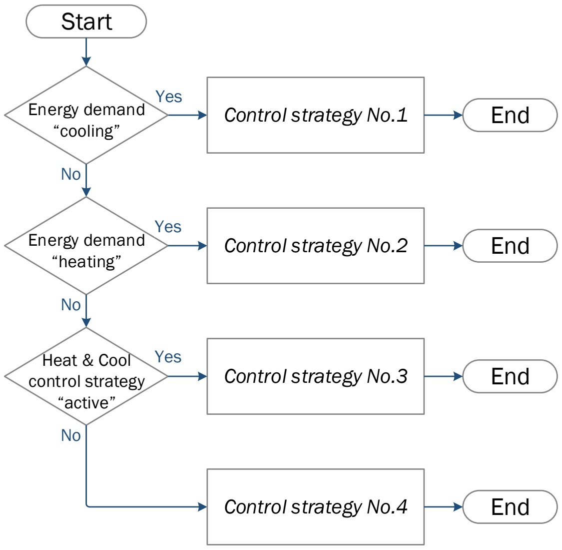

Figure 7: Flow Chart of the considered control strategy of the external shading devices

Each of the four displayed control strategies (No. 1 to No. 4) in Figure 7 have different impacts on the position of the blinds (due to different parameters for the height of shading and the slat angle of the blinds) but all ensure glare protection of the building occupants. Therefore the angle β_{critic} can be calculated with the geometrical information of the blinds, the orientation of the glass façade and the position of the sun (relative azimuth angle of the façade, elevation of the sun, angle of incidence). The following functions will be used for the calculation of the height of the shading and for the slat anlge of the blinds:

$$\textit{height}=f(\ \gamma_{facade};\ \bar{I}_{G,F,90};\ \bar{T}_{Room};\ \bar{T}_{Ambient};\ T_{SET;R,heating};\ T_{SET;R,cooling};\ \Delta T_{SET;R}\ )$$

$$\textit{slat angle}=f(\ \gamma_{facade};\ \bar{I}_{G,F,90};\ \bar{I}_{D,H}\ /\ \bar{I}_{G,H};\ \bar{T}_{Room};\ \bar{T}_{Ambient};\ T_{SET;R,heating};\ T_{SET;R,cooling};\ \Delta T_{SET;R};\ \beta_{critic}\ )$$

The calculation interval for the mean values of the temperatures and the solar irradiation is a user input in the graphical user interface for the shading devices. It can also be seen that the set values of the room air temperature for heating ($T_{SET;R;heating}$) or cooling ($T_{SET;R;cooling}$) have an impact on the setting of the blinds. Therefore, the activation of the cooling system takes place when the room air temperature increases despite the maximum height of the shading device with the optimized slat angle (at least equal to β_{critic}).

BOUNDARY CONDITIONS

Weather conditions changed during the investigations or optimization. Therefore the installed weather station and the implemented cloud-based measurement data acquisition system to evaluate the weather conditions was used. In the following Figure 8 the daily average outside ambient temperature and also the global horizontal irradiance is shown. The displayed data gap from May 2018 to the middle of June 2018 was closed with data from the subsequent period, from mid-June 2018 to July 2018. The annual average outside ambient temperature from 03/2018 to 02/2019 is about 11.37°C and from 03/2019 to 02/2020 about 11.27°C. Also the summarized global horizontal irradiance from 2018 to 2019 is about $I_{global;2018}$=1,321 kWh/m² and from 2019 to 2020 about $I_{global;2019}$=1,223 kWh/m².

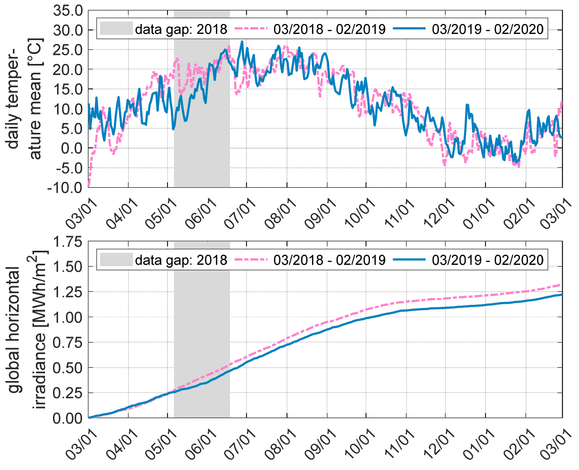

Figure 8: Daily average outside ambient temperature (top) and global horizontal irradiance (bottom) at the study location (Pinkafeld, Austria) from 03/2018 to 02/2020

The calculated heating degree days (HDD) and cooling degree hours (CDH) are listed in Table 2 and Table 3. A comparison of the indicators of the two time periods shows that from 2019 to 2020 the heating degree days are up to 4% higher than the values from

DOI: 10.3217/978-3-85125-786-1-40

2018 to 2019, depending on the reference temperature. In contrast to this the cooling degree hours from 2019 to 2020 are up to 12% lower than the values from 2018 to 2019.

Table 2:
Heating degree days (HDD) with two different room air temperatures (subscript)

	03/2018 – 02/2019	03/2019 – 02/2020
$HDD_{20/12}$	2,913 K·d	2,965 K·d
$HDD_{22/12}$	3,268 K·d	3,373 K·d

Table 3:
Cooling degree hours (CDH) with two different reference temperatures (subscript)

	03/2018 – 02/2019	03/2019 – 02/2020
$CDH_{18.3}$	10,105 K·h	8,897 K·h
$CDH_{20.0}$	6,749 K·h	6,011 K·h

RESULTS

The next subsections present a comparison between the experimental data from 03/2018 to 02/2019 and the experimental data from 03/2019 to 02/2020. Because of the character of the building, implementation of all measures was not complete until July 2019, therefore not all the measures and their impacts took effect in March 2019.

Room air temperature

The control strategies for space heating and cooling and also for the external shading devices influences the distribution of the room air temperature. Figure 9 shows the histogram of the room air temperatures of the ground floor and Figure 10 of the upper floor. In both figures, a bimodal distribution of the room air temperatures become apparent after taken measures.

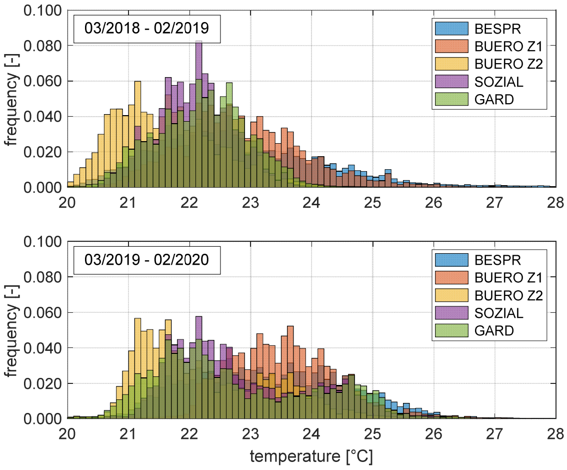

Figure 9: Histogram of room air temperatures (legend: specific room names), ground floor (top: 03/2018-02/2019; bottom: 03/2019-02/2020)

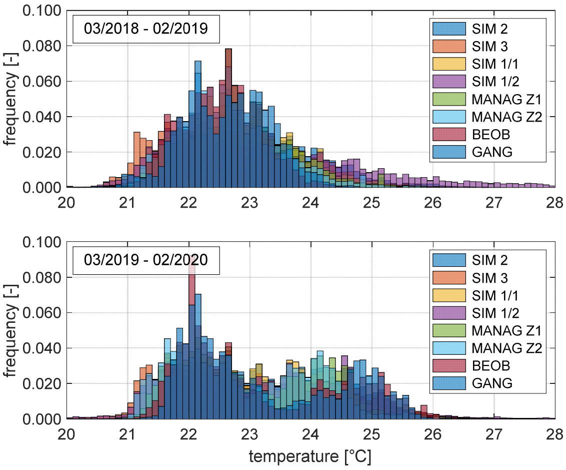

Figure 10: Histogram of room air temperatures (legend: specific room names), upper floor (top: 03/2018-02/2019; bottom: 03/2019-02/2020)

Space Heating

The comparison of the monthly energy demand for space heating with the activated static heating surfaces is shown in Figure 11. The total energy demand for space heating is slightly increased, from 17,463 kWh/a to 18,726 kWh/a. One reason of this is the increased number of heating degrees days (cf. Table 2).

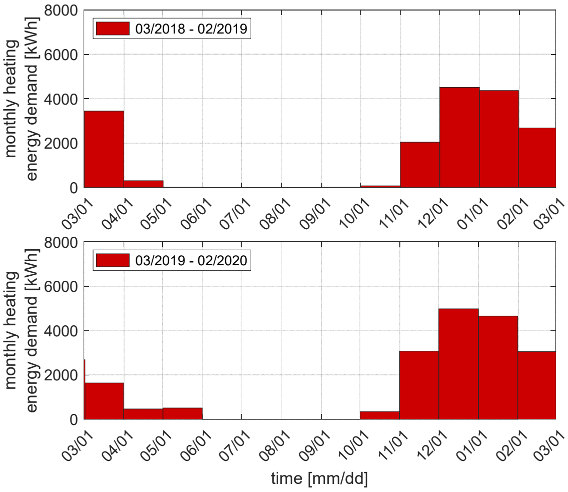

Figure 11: Monthly energy demand for space heating (with static heating surfaces) (top: 03/2018-02/2019; bottom: 03/2019-02/2020)

Space Cooling

Figure 12 shows the comparison of the monthly energy demand for space cooling with the activated static cooling surfaces. The actions taken caused a dramatic decrease in the energy demand for space cooling, from a total of 18,282 kWh/a to 5,461 kWh/a. Despite the reduction of the cooling degree hours, (cf. Table 3) the main part of the reduction can be attributed to the strictly implemented control strategy for the external shading devices.

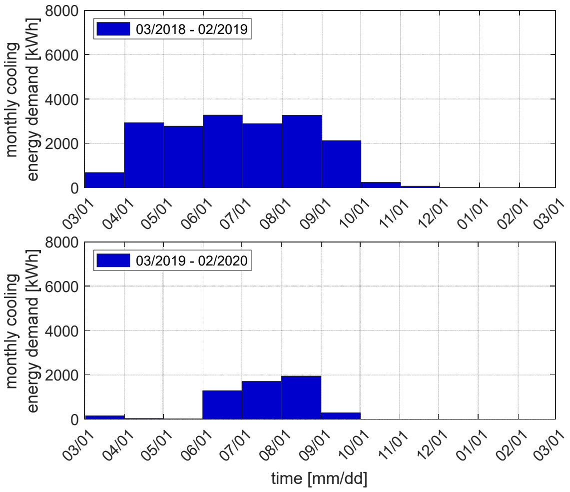

Figure 12: Monthly energy demand for space cooling (with static cooling surfaces) (top: 03/2018-02/2019; bottom: 03/2019-02/2020)

Air conditioning system

The evaluation of the monthly energy demand for heating and cooling (and/or dehumidification) through the air conditioning system is displayed in Figure 13. While the total energy demand for heating decreased from 18,187 kWh/a to 7,151 kWh/a, the total energy demand for cooling (and/or dehumidification) decreased from 12,224 kWh/a to 2,496 kWh/a. The demand reduction can be attributed to the set value for dehumidification, the adapted operating schedule and the change of the control parameter from relative to absolute humidity.

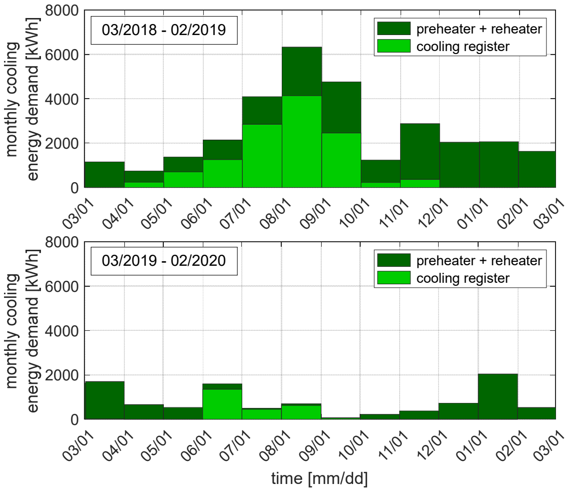

Figure 13: Monthly energy demand for the preheater and reheater and for the cooling register of the air conditioning system (top: 03/2018-02/2019; bottom: 03/2019-02/2020)

The distribution of the supply air temperature is shown in Figure 14 and the distribution of the relative humidity of the exhaust air in Figure 15. In both Figures the impact of the new defined set values are recognizable (e.g. dehumidification at 60%rH).

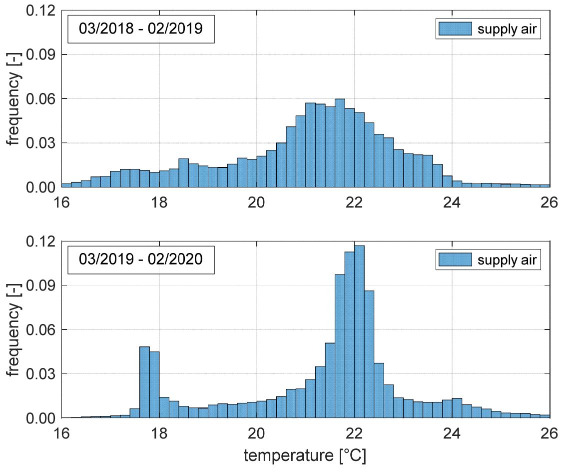

Figure 14: Distribution of the supply air temperature of the air conditioning system (top: 03/2018-02/2019; bottom: 03/2019-02/2020)

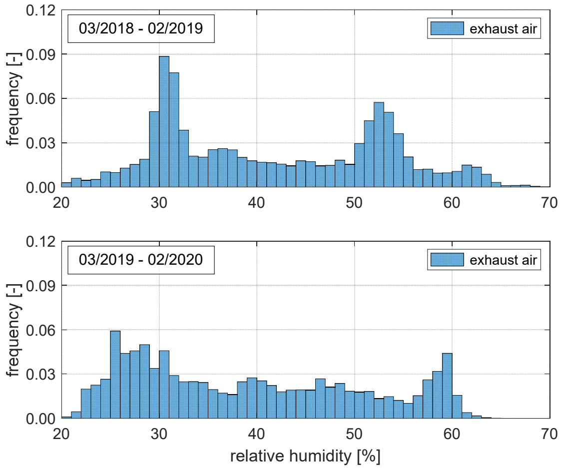

Figure 15: Distribution of the relative humidity of the exhaust air (top: 03/2018-02/2019; bottom: 03/2019-02/2020)

Electrical energy demand for lighting

To evaluate the control strategy for the external shading devices in terms of daylight utilization, Figure 16 compares the electrical energy demand for lighting the office rooms in the upper floor of the ENERGETIKUM (SIM 2; SIM 3; SIM 1/1 and SIM 1/2). Total electricity for lighting decreased from 1,267 kWh/a to 638 kWh/a. Possible reasons for this substantial reduction are a change of the room occupation and also the newly implemented control strategy for the external shading devices.

DOI: 10.3217/978-3-85125-786-1-40

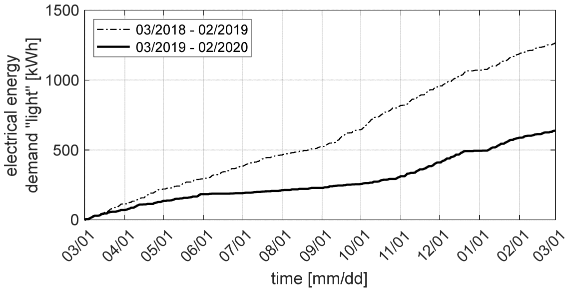

Figure 16: Integrated electricity demand for lighting the office rooms SIM 1/1; SIM 1/2; SIM 2 and SIM 3.

Total electrical energy demand

Finally the comparison of the total electrical energy demand (with and without the demand for the building's reversible heat pump) is shown in Figure 17. Due to the reduction of the energy demand for space cooling and for dehumidification/cooling of the supply air, the total electricity demand for the reversible heat pump also decreased, from 13,461 kWh/a to 6,145 kWh/a. Also, the electrical energy demand of all other energy consuming devices was reduced from 46,862 kWh/a to 43,150 kWh/a. The main aspect of this savings can be accounted for by a lower electricity demand by lighting, pumps and fans.

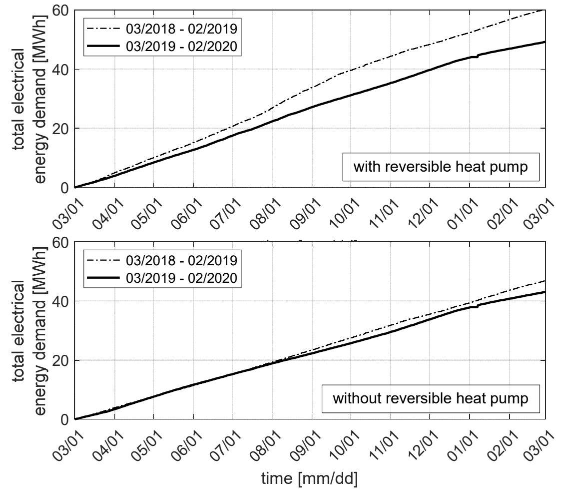

Figure 17: Integrated demand of electrical energy (top: with reversible heat pump; bottom: without reversible heat pump).

CONCLUSION

To identify the energy savings potential of an office building with glass façades and with static heating and cooling surfaces, an investigation was conducted on a living laboratory building (office building under real-life operating conditions). These investigations were prompted by a prior analysis of the operating behaviour of the different technical building devices with findings similar to that of Fuetterer et al. (2017) (cf. Waide (2013)).

The BACnet-OPC Matlab user interface developed as part of this work includes an intelligent control strategy of the external shading devices, a control strategy for the static heating and cooling surfaces and a control strategy for the hygienic air change in all thermal zones and was shown to be viable. Furthermore, the air conditioning system was manually optimized (changing of control parameters, set values, control variable, time schedule). The BACnet-OPC Matlab user interface has been operational for more than 18 months, controlling the above-mentioned technical building equipment in the living laboratory ENERGETIKUM under real-life operating conditions. The overall energetic impacts of the implemented measures are listed in Table 4.

Table 4:
Yearly energy demand and evaluation of the energy demand reduction

SYSTEM	**03/2018 – 02/2019 [kWh]**	**03/2019 – 02/2020 [kWh]**	**Δ [%]**
Space heating	17,463	18,726	+7.2
Space cooling	18,282	5,461	-70.1
Ventilation: preheater and reheater	18,187	7,151	-60.7
Ventilation: cooling register	12,224	2,496	-79.6
Electricity for reversible heat pump	13,461	6,145	-54.3
Electricity (without reversible heat pump)	46,862	43,150	-7.9

These long-term experimental investigations have demonstrated that the proposed control strategy can dramatically reduce the energy demand of the building and improve the thermal impacts of the building occupants' behaviour. In the next months, further investigations with an extended version of the BACnet-OPC Matlab user interface should clarify the energy savings potential of model predictive control algorithm (MPC algorithm) and also the demand side flexibility (grid connectivity) of the living laboratory building.

ACKNOWLEDGEMENT

This work has received funding from the Federal Ministry for Digital and Economic Affairs (BMDW) within the funding scheme COIN – "Network" (8th Call) managed by FFG under grant agreement No. 855979 (acronym "ZGEM") and the funding scheme COIN – "Aufbau" (capacity building) (6th Call) managed by FFG under grant agreement No. 856371 (acronym "EDMA").

REFERENCES

Bernardo, H., Leitão, S., Neves, L., Rodrigues, P. 2010. Assessment of the energy savings potential of daylight utilization and its impact on a building energy performance, Third German-Austrian IBPSA Conference Vienna University of Technology, BauSIM2010, http://info.tuwien.ac.at/bausim/conftool/bernardo-2010-assessment_of_the_energy_savings_potential_of_daylight_utilization_and_its_impact_on_a_building_energy.pdf

European Commission. 2018. Directive (EU) 2018/844 of the European Parliament and of the Council of 30 May 2018 amending Directive 2010/31/EU on the energy performance of buildings and Directive 2012/27/EU on energy efficiency, Official Journal of the European Union, https://eur-lex.europa.eu/legal-content/EN/TXT/PDF/?uri=CELEX:32018L0844&from=EN

Fütterer, J., Schild, T., Müller D. 2017. Gebäudeautomationssysteme in der Praxis, Whitepaper RWTH-EBC 2017-001, Aachen, http://dx.doi.org/10.18154/RWTH-2017-05671

Karasu, A., Steffan, C. 2010. Building energy performance simulations of the residential houses in mediterranean climate: case study for Bodrum, Turkey, Third German-Austrian IBPSA Conference Vienna University of Technology, BauSIM2010, http://info.tuwien.ac.at/bausim/conftool/karasu-2010-building_energy_performance_simulations-172.pdf

Klanatsky, P., Plank, H., Heschl, Ch. 2019a. Die „smarte“ Fassade zur Optimierung des Energiebedarfs und thermischen Komforts. Präsentation. 23. Internationaler Wissenschaftskongress e·nova, Fachhochschule Burgenland GmbH, Studienzentrum Pinkafeld, Austria, 21.-22. Nov. 2019

Klanatsky, P., Plank, H., Heschl, Ch. 2019b. Development of an innovative blind control strategy to increase the thermal comfort of an office building. 10th International conference: Indoor Climate of Buildings, ICB2019, Nový Smokovec, Slovakia, 8.-11. Dec. 2019

Nasrollahi, F. 2010. Window area in office buildings from the viewpoint of energy efficiency, Third German-Austrian IBPSA Conference Vienna University of Technology, BauSIM2010, http://info.tuwien.ac.at/bausim/conftool/nasrollahi-2010-window_area_in_office_buildings_from_the_viewpoint-180.pdf

Planas, C., Cuerva, E., Alavedra, P. 2018. Effects of the type of facade on the energy performance of office buildings representative of the city of Barcelona, Ain Shams Engineering Journal, Vol. 9, pp. 3325-3334

Plank, H., Klanatsky, P., Veynandt, F., Stelzer, R., Traunmüller, W. 2019. Solar radiation as a building control parameter – A comparison of measured and predicted values. 10th International conference: Indoor Climate of Buildings, ICB2019, Nový Smokovec, Slovakia, 8.-11. Dec. 2019

Sagerschnig, C., Seerig, A., Dietrich, C. 2010. Die Gebäudehülle als aktives Bauteil: Optimierung der Interaktion von Gebäudetechnik und Sonnenschutzsteuerung, Third German-Austrian IBPSA Conference Vienna University of Technology, BauSIM2010, http://info.tuwien.ac.at/bausim/conftool/seerig-2010-die_gebaeudehuelle_als_aktives_bauteil-129.pdf

Tzempelikos, A., Shen, H. 2011. Daylighting and energy analysis of private offices with automated interior roller shades. Sol Energy, Solar Energy, Vol. 86, Issue 2; pp. 681-704

Waide Strategic Efficiency, 2013. The scope for energy and CO2 savings in the EU through the use of building automation technology: Final report, 10 August 2013

Westphal, F. S., Andreis, C. 2016. Influence of Glazed Façades on Energy Consumption for Air Conditioning of Office Buildings in Brazilian Climates, International Journal of Engineering Research and Application, Vol. 6, Issue 11, Part 1, pp. 54-60

DOI: 10.3217/978-3-85125-786-1-40